

# A cathodoluminescent sol–gel material

S. M. JONES, L. KOTORMAN\*, S. E. FRIBERG

*Departments of Chemistry and \*Physics, Center for Advanced Materials Processing, Clarkson University, Potsdam, NY 13676, USA*

Cerium activated  $Y_2SiO_4$ , a fast, blue emitting phosphor, was incorporated into a composite organic/inorganic polymeric material. The phosphor was added to an initial system of tetraethoxysilane, water (w/ $HNO_3$ ), methylmethacrylate and ethanol, and the mixture was then allowed to undergo hydrolysis and condensation. Prior to the condensation, the phosphor settled to the bottom of the container and was firmly bonded to the surface of the resultant glass. The cathodoluminescence and the luminescent decay of the excited phosphor were observed. The fact that the phosphor was bound to the glass did not poison its luminescence and the decay time was found to be 75 ns.

## 1. Introduction

The sol–gel method exhibits several advantages over classical glass processing stemming primarily from the fact that the initial system begins as a liquid mixture and subsequently forms an  $SiO_2$  network upon standing [1–3]. This means that glasses of very high purity and homogeneity can be achieved and also that the processing can be done at room temperature. These processing parameters have led to the possibility of producing glasses which are uniformly doped with organic molecules, such as laser dyes, e.g. xanthene dyes, oxazines and coumarins. The photoluminescent properties of the doped glasses have been thoroughly documented over the past decade [4–9]. It has been suggested that these glasses could be used as dye laser components [10–13], solar energy concentrators [10, 11] and particle detectors [14–16].

There is currently a great deal of interest in producing novel electroluminescent and cathodoluminescent materials, which could be used as particle detectors. Doped organic polymers are presently used as particle detectors. Despite the fact that glass scintillators display certain advantages over plastics, such as thermal stability, higher density, and insensitivity to ambient radiation, they have not been widely used since it is difficult to dope glasses properly. The standard method of applying inorganic phosphors to glasses is to form a slurry of the phosphor which is then spread over the glass and allowed to dry. However, the application of the phosphor is to the surface of the glass only, and it is easily removed if the glass is not handled with extreme care. Since sol–gel materials are formed from a liquid precursor, the inorganic phosphor can be added to the initial system, settles out of the liquid precursor and is subsequently incorporated into the surface of the resultant material as the  $SiO_2$  network forms. In this way, the phosphor would form a thin layer on the  $SiO_2$  surface while being bound to the network and yet would still exhibit cathodoluminescence. This is very desirable for good

heat transfer between the phosphor and the glass, especially in the case of high intensity applications. Organic monomer was added and subsequently polymerized to strengthen the final material, reducing the brittleness of the final glass [17, 18].

## 2. Experimental procedure

### 2.1. Materials

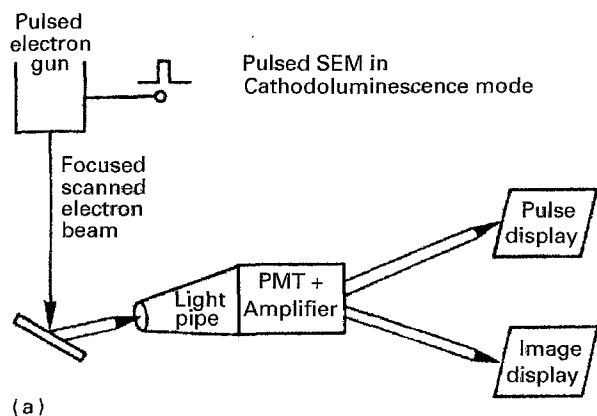
Tetraethoxysilane (TEOS > 99%), ethanol (95%), nitric acid, methyl methacrylate, 2,2'-azobis(2-methylpropionitrile) and yttrium aluminium silicate ( $Y_2SiO_4$ ) were all used as received.

### 2.2. Sample preparation

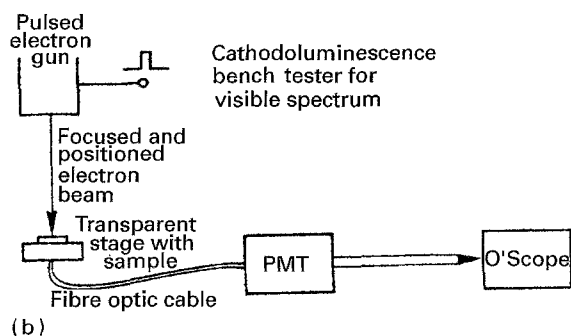
The TEOS, water (pH 1 w/ $HNO_3$ ), and ethanol were mixed forming a transparent system. Methyl methacrylate and an initiator, 2,2'-azobis(2-methylpropionitrile), which had been mixed together, were then added. The phosphor,  $Y_2SiO_4$ , was then added and the mixture was poured into a disposable plastic sample dish and covered. After two weeks the cover was removed and the samples were placed in an ultraviolet chamber and irradiated for six hours to polymerize the methyl methacrylate in the system. The final host material was composed of a mixture of  $SiO_2$ , resulting from the hydrolysis and the condensation of the TEOS, and polymethyl methacrylate.

### 2.3. Scanning electron microscopy and excitation decay times

The cathodoluminescent micrograph and the secondary electron micrograph accompanying it (Figs 4, 5, and 6) were taken on a modified ISI Model DS 130 scanning electron microscope (SEM) fitted with a cathodoluminescence detector (see Fig. 1(a)). A Jeol Model 6300 SEM with a Noran Instruments Voyager X-ray microanalyser was used to produce other



(a)



(b)

Figure 1 Block diagrams of the pulsed SEM in cathodoluminescent mode (a) and the cathodoluminescence bench tester for visible spectrum (b).

TABLE I Cathodoluminescent sample compositions (g)

Sample	TEOS	Water	Ethanol	MMA	Y <sub>2</sub> SiO <sub>4</sub>
CL4	1.801	0.558	0.902	0.404	0.037
CL5	3.114	0.778	1.351	0.552	0.161

secondary electron micrographs (Figs 2, 3, 7, and 9) and the elemental analysis displays (Figs 9 and 11).

The excitation decay times were observed on an instrument assembled in the laboratory by the authors. The instrument included a vacuum chamber with a pulsed electron gun and a fibreoptics/photo-multiplier-based detection system for the measurement of fluorescence decay (see Fig. 1(b)). The pulse and decay signals were displayed on an oscilloscope screen which was then photographed.

### 3. Results

The initial composition, in grams, of the samples are given in Table I. The density of the phosphor particles in the bulk region of the doped layer for sample CL5 was calculated to be  $1 \text{ mg cm}^{-2}$ .

Fig. 2 is a scanning electron micrograph showing the phosphor particles bound to the surface of the SiO<sub>2</sub> network of sample CL4. The size of the phosphor particles can be seen to be 1–2  $\mu\text{m}$ . Fig. 3 is a scanning electron micrograph of a cross-section of the outer layer of silicate of sample CL5 containing the phosphor particles. The dark area to the right of the picture is the undoped silicate, while the mottled

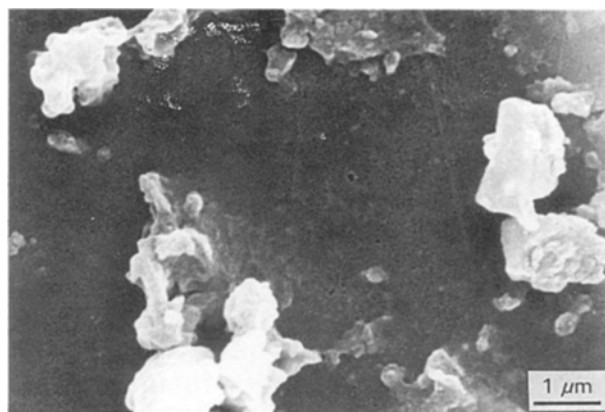


Figure 2 Scanning electron micrograph of phosphor particles partially embedded in the SiO<sub>2</sub> network of sample CL4.

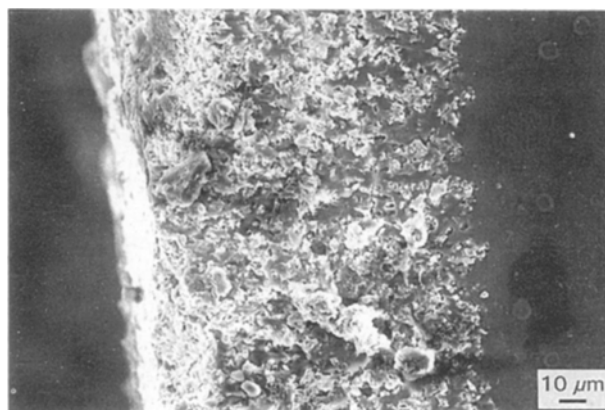


Figure 3 Scanning electron micrograph of the cross-section of the phosphor containing layer on the surface of sample CL5.

region is where the phosphor has been incorporated into the host material. The bright region to the left is the true outer surface of the sample which is facing off to the left in this picture. The thickness of the phosphor layer was approximately 0.1 mm for sample CL5.

Sample CL4 was placed in a modified ISI SEM and a photograph was taken using the secondary electrons (Fig. 4). A photograph was also taken using the photons given off from the cathodoluminescence (Fig. 5). Note that the photographs shown in Figs 4 and 5 were taken of the same area of the same sample with only a slight shift of perspective.

Secondary electron photographs and cathodoluminescent photographs (Figs 6 and 7, respectively) were taken of a piece of sample CL5 shortly after removing the sample from the u.v. chamber, i.e. two weeks after preparation. The sample formed a network of microcracks on the surface when placed at very low pressure, while the sample maintained its overall integrity. The luminescence at this point in time can be seen to be almost exclusively from the areas immediately around the cracks and yet involves much more of the surface than for sample CL4. The bright areas in the cathodoluminescent images are due exclusively to emitted photons, while the increased brightness of the areas around the microcracks in Fig. 5 is due to charging of these areas and may be due to changes in surface conduction and the increased voltage used.

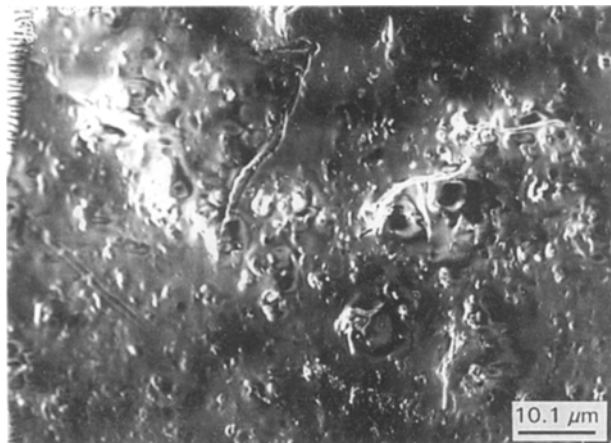


Figure 4 Secondary electron micrograph of sample CL4 surface.

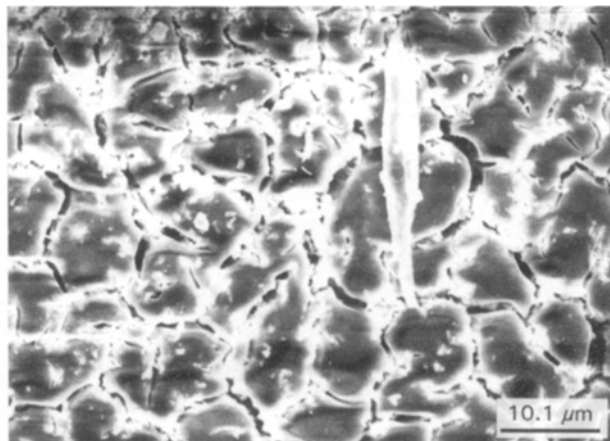


Figure 6 Secondary electron micrograph of sample CL5 surface showing the presence of embedded phosphor particles and micro-cracking.

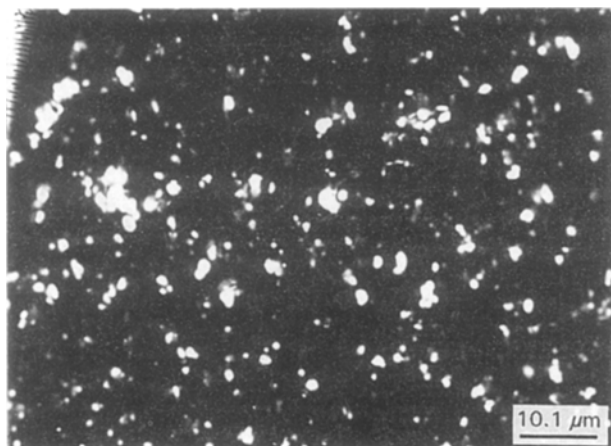


Figure 5 Cathodoluminescent micrograph of the same surface area of sample CL4 as that shown in Fig. 2.

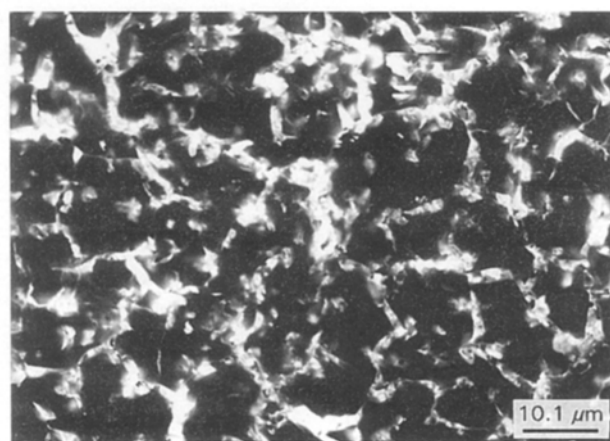


Figure 7 Cathodoluminescent micrograph of the same surface area of sample CL5 as that shown in Fig. 4.

Fig. 8 is a scanning electron micrograph of the surface of sample CL5, showing, once again, the phosphor particles trapped in the silicate host. Fig. 9 is the elemental analysis display of the surface area shown in Fig. 8 of sample CL5 after it had dried for eight weeks after removal from the u.v. chamber. The amount of the phosphor can be seen to be quite low relative to that of the silicate. Fig. 10 is a scanning electron micrograph of a region of sample CL5 after approximately ten  $\mu\text{m}$  of the outer surface had been removed. Fig. 11 is the elemental analysis of the region shown in Fig. 10. When compared to Fig. 8 the amount of phosphor is clearly much greater. It should be noted that the electron beam energy was 10 kV for sample CL4, while it was 15 or 19 kV for sample CL5. This difference may affect the intensity slightly, but would not affect the extent of the luminescent areas observed since the photons detected were those given off on the same side of the sample which was struck by the excitation beam. Therefore, factors such as the penetration depth of the beam and interference effects do not have to be taken into consideration.

Sample CL4 was placed in a vacuum chamber which was pumped down to  $1.333 \times 10^{-5}$  Pa. The sample was then excited with an electron beam and the resultant cathodoluminescent emission was

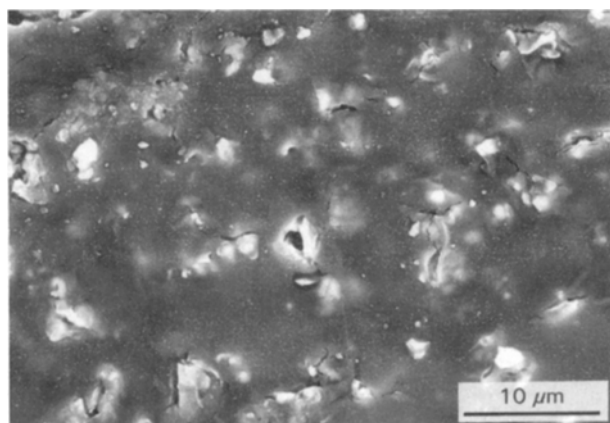


Figure 8 Scanning electron micrograph of the outer surface of sample CL5.

observed. The electron beam was pulsed and the resultant decay of the cathodoluminescence was recorded (Fig. 12). The luminescent decay time was approximately 75 ns.

#### 4. Discussion

Figs 2, 3, and 4 illustrate the fact that the phosphor is firmly bound by the  $\text{SiO}_2$  network. In Fig. 2 several of

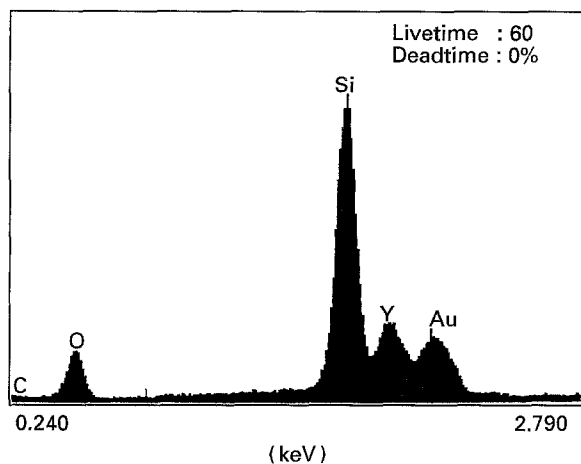


Figure 9 Elemental analysis spectrum of the area shown in Fig. 7 of the outer surface of sample CL5 formed by the condensing silanols.

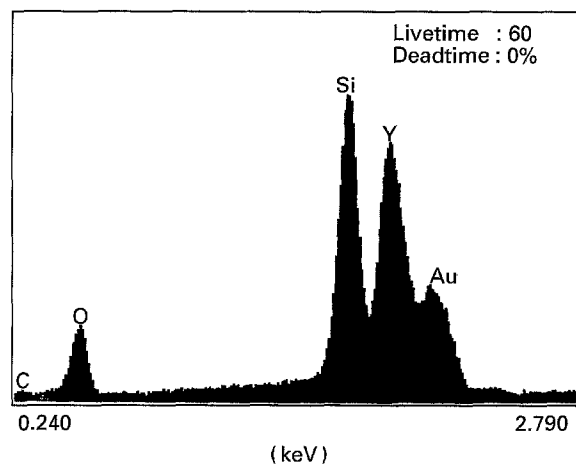


Figure 11 Elemental analysis spectrum of the area shown in Fig. 9 of sample CL5 after removal of the outer twenty  $\mu\text{m}$  of the naturally occurring phosphor doped, silicate surface.

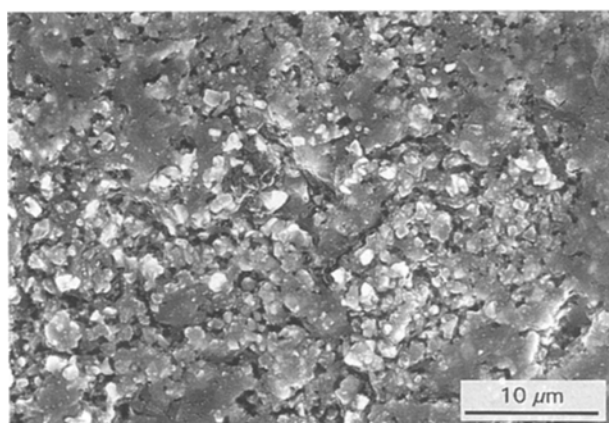


Figure 10 Scanning electron micrograph of the phosphor-doped layer after removal of approximately 20  $\mu\text{m}$  of the outer surface from sample CL5.

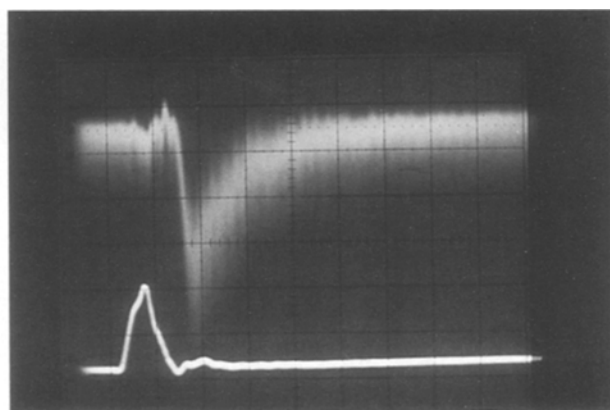


Figure 12 Excitation and relaxation of  $\text{Y}_2\text{SiO}_4$  bound to sol-gel glass.

the phosphor particles can be seen to be partially embedded in the  $\text{SiO}_2$  network, while still presenting an exposed portion which proved to be cathodoluminescent. The cathodoluminescent micrograph, Fig. 5, shows the distribution of the emitting phosphor particles over the surface of the glass. The surface coverage of emitting phosphor particles is approximately 10%. This is relatively low, but it was believed that this could be increased by adding more phosphor to the precursor mixture. However, when more phosphor was added and the sample was placed in the evacuated environment of the SEM before thorough drying the sample formed microcracks (see Fig. 6). It is of interest that the strongest luminescence is seen to be concentrated in and around these cracks, (Fig. 7). The condensing silanols appear to have formed a layer on the exterior of the sample which contains some phosphor. Non-luminescent surface layers have been considered by Yaun *et al.* [19] in that they present a complication to the standard theories used to model cathodoluminescent thin films. However, it appears that there is a region, very rich in phosphor lying below the surface of the sample which is exposed by the cracking. This subsurface region is then also involved in the luminescence upon being exposed by the cracking. The result

of this is that the overall luminescence is increased due to the exposure of additional phosphor.

Sample CL5 was then allowed to dry thoroughly and  $\sim 20 \mu\text{m}$  of the outer surface was removed. By comparing Figs 8 and 9 with Figs 10 and 11, respectively, one can see that there is indeed a region which is very rich in phosphor lying below the outer surface. This is clearly demonstrated by the increase in the yttrium content as shown by Fig. 11. The fact that there is a primarily silicate outer surface is not surprising since this surface formed at the bottom of the container in which the sample condensed. The phosphor particles were 1–2  $\mu\text{m}$  in diameter and thus the condensing silanols in the surrounding liquid enveloped most of the particles before forming the solid silicate network. When this surface is removed the densely packed phosphor particles are exposed. This in itself could prove to be a processing advantage in that it would provide a means of achieving homogeneous, low density surface coverage. Homogeneous, low density surface coverages are difficult to produce by means of sedimentation and evaporation techniques [20, 21]. Surface coverage density is an important experimental parameter since it has been shown that low densities, i.e.  $1 \text{ mg cm}^{-2}$  are the most efficient for 2–3  $\mu\text{m}$  size phosphor particles [20]. The phosphor

can be added such that it saturates the outer silicate region, since adding more phosphor merely creates a thicker layer and not a denser layer. After the removal of a portion of the outer layer, by cutting with a microtome or possibly by grinding, the resultant layer could be processed to any desired thickness. This also means that in microcracking that may occur when the sample is placed under low pressure is not a problem since the surface layer is subsequently removed. Since the density of the phosphor particles appears to taper off as the interior silicate material is approached, the surface density could be tailored by removal of an appropriate amount of the outer layer. Yet, the homogeneity of the surface density of the phosphor particles would not be affected by this processing. However, it must be noted that the processing (e.g. grinding) of phosphor particles can influence their luminescence. So care must be taken not to poison, in some way, their luminescent properties by any processing subsequent to their being embedded in the silicate host.

Fig. 12 shows that the cathodoluminescent emission of the sample was relatively strong and that the phosphor was not poisoned when incorporated in the surface of the SiO<sub>2</sub> network. The observed lifetime of the phosphor in the sample is 75 ns, which is approximately the same as that of the pure phosphor. The emission from the sample was in the blue wavelength region, which is typical of Ce-activated yttrium silicates [22] and displayed uniformity across the surface of the sample. This result also shows that this method could be used for cathodoluminescent displays since the emitted light was created in the phosphor layer and then passed through the transparent, undoped silicate formed where it was then observed.

The advantages offered by the sol-gel method have been shown to be of use in the production of a novel cathodoluminescent material. The fact that the initial system was a condensing liquid and produced a homogeneous phosphor region, since inhomogeneities in phosphor distribution become a problem at low surface densities for sedimentation techniques [21]. The method presented here also does not require a binder such as Na<sub>2</sub>SiO<sub>3</sub>, in that the silicate network acts to bind the phosphor to the surface and within the underlying silicate network. By employing this method

one can produce thin cathodoluminescent layers on substrates which can be processed to any desired thickness.

## References

1. J. C. BRINKER and G. W. SCHERER, "Sol-gel science, the physics and chemistry of sol-gel processing" (Academic Press, New York, 1990).
2. L. L. HENCH and J. K. WEST, *Chem. Rev.* **90** (1990) 33.
3. J. LIVAGE and C. SANCHEZ, *J. Non-Cryst. Solids* **145** (1990) 11.
4. D. LEVY, R. REISFELD and D. AVNIR, *Chem. Phys. Lett.* **109** (1984) 593.
5. J. MCKEIRNAN, J. C. POUXVIEL, B. DUNN and J. I. ZINK, *J. Phys. Chem.* **93** (1989) 212.
6. K. MATSUI, T. MATSUZUKI and H. FUJITA, *Ibid.* **93** (1989) 4991.
7. D. LEVY and D. AVNIR, *Ibid.* **92** (1988) 4934.
8. D. LEVY, S. EINHORN and D. AVNIR, *J. Non-Cryst. Solids* **113** (1989) 137.
9. D. PRESTON, J.-C. POUXVIEL, T. NOVINSON, W. C. KASKA, B. DUNN and J. I. ZINK, *J. Phys. Chem.* **94** (1990) 4167.
10. R. REISFELD, *J. Non-Cryst. Solids* **121** (1990) 254.
11. R. REISFELD, D. BRUSILOVSKY, M. EGAL, E. MIRON, Z. BURSTEIN and J. IRVI, *Chem. Phys. Lett.* **160** (1989) 43.
12. E. T. KNOBBE, B. DUNN, P. D. FUGUA and F. NISHIDA, *Appl. Opt.* **29** (1990) 2729.
13. J. M. MCKEIRNAN, S. A. YAMANAKA, B. DUNN and J. I. ZINK, *J. Phys. Chem.* **94** (1990) 5653.
14. J.-L. NOGUES and W. V. MORESHEAD, *J. Non-Cryst. Solids* **121** (1990) 136.
15. J.-L. NOGUES, S. MAJEWSKI, J. K. WALKER, M. BOWEN, R. WOJCIK and W. V. MORESHEAD, *J. Amer. Ceram. Soc.* **71** (1988) 1159.
16. L. L. HENCH, J. K. WEST, B. F. ZHU and R. OCHOA, in SPIE, Vol. 1328, "Sol-gel optics", (1990) p. 230.
17. S. E. FRIBERG, C. C. YANG, M. B. BISCOGLIO and H. HELBIG, *J. Mater. Sci.* **11** (1992) 1173.
18. E. J. A. POPE, A. ASAMI and J. D. MACKENZIE, *J. Mater. Res.* **4** (1989) 1018.
19. J. YUAN, S. D. BERGER and L. M. BROWN, *J. Phys., Cond. Matter* **1** (1989) 3253.
20. G. E. GIAKOUMAKIS, C. D. NOMICOS and P. C. EUTHYMIU, *Can. J. Phys.* **59** (1980) 88.
21. *Idem.* *J. Appl. Phys.* **51** (1980) 4976.
22. S. SHMULOVICH, G. W. BERKSTRESSER, C. D. BRANDLE and A. VALENTINO, *J. Electrochem. Soc.* **135** (1988) 3141.

Received 8 November 1994  
and accepted 8 September 1995